

Enhanced photoacoustic detection using photonic crystal substrate

Yunfei Zhao,¹ Kaiyang Liu,¹ John McClelland,^{2,3,4} and Meng Lu^{1,3,a)}

¹Department of Electrical and Computer Engineering, Iowa State University, Ames, Iowa 50011, USA

²Ames Laboratory-USDOE, Ames, Iowa 50011, USA

³Department of Mechanical Engineering, Iowa State University, Ames, Iowa 50011, USA

⁴Department of Biochemistry, Biophysics, and Molecular Biology, Iowa State University, Ames, Iowa 50011, USA

(Received 27 February 2014; accepted 9 April 2014; published online 23 April 2014)

This paper demonstrates the enhanced photoacoustic sensing of surface-bound light absorbing molecules and metal nanoparticles using a one-dimensional photonic crystal (PC) substrate. The PC structure functions as an optical resonator at the wavelength where the analyte absorption is strong. The optical resonance of the PC sensor provides an intensified evanescent field with respect to the excitation light source and results in enhanced optical absorption by surface-immobilized samples. For the analysis of a light absorbing dye deposited on the PC surface, the intensity of photoacoustic signal was enhanced by more than 10-fold in comparison to an unpatterned acrylic substrate. The technique was also applied to detect gold nanorods and exhibited more than 40 times stronger photoacoustic signals. The demonstrated approach represents a potential path towards single molecule absorption spectroscopy with greater performance and inexpensive instrumentation. © 2014 AIP Publishing LLC. [<http://dx.doi.org/10.1063/1.4872319>]

Photoacoustic (PA) spectroscopy has attracted great interest since the mid-1970s due to its capability to non-invasively monitor light absorbing analytes over substantial ranges of concentrations.^{1–4} Although laser-based PA detections exhibit a higher sensitivity as compared to optical absorption measured directly by transmission spectroscopy, it is always desirable to improve the signal-to-noise ratio to accurately quantify trace amounts of molecules. To maximize the signal-to-noise ratio of PA measurements, a variety of approaches have been studied for the purpose of amplifying acoustic output and suppressing noise. The reported signal enhancements arise from two major effects: acoustic resonance and optical resonance.^{5–9} Notably, optical resonance-based methods utilize cavities, formed by high reflectivity mirrors or micro-/nanostructures, to increase optical path length and to result in enhanced absorption by the target molecule residing inside the cavity.¹⁰

To address the challenge of measuring solid substance at low concentrations or with low absorption coefficient, we propose to use a one-dimensional photonic crystal (PC) structure to increase light absorption and to generate a stronger PA output consequently. The PC substrate, comprised of a periodically nanostructured dielectric thin film, supports guided-mode resonance (GMR), also known as a leaky mode.^{11–13} The GMR effect occurs when the PC substrate is illuminated under resonance conditions and leads to intensified local field with respect to the electric field strength of the incident light. By spectrally overlapping a GMR resonance wavelength with the absorption band of the analyte, one can obtain an increase in the optical absorption. Previous publications have demonstrated the application of a PC substrate for fluorescence-based detections.^{14–17} Several compelling features of the PC are of practical importance for the development of an enhanced detection scheme to be used in PA

analysis. The PC structure can be tailored to tune the GMR wavelength from visible to mid-infrared, and thus the GMR wavelength can align with the absorption bands of a wide variety of substances.^{18–20} It is inexpensive to fabricate large surface areas of PC substrates using optically transparent materials and to incorporate them into a PA detection instrument. In addition, the PC substrate is made using polymer material with low thermal conductivity that prevents heat dissipation and ensures strong PA signal output. This Letter reports design and experimental characterization of a PC sensor for enhanced PA detection of organic dye molecules and metal nanoparticles (NPs).

A cross-sectional diagram (not to scale) of the PC structure adopted for the PA experiment is shown in Fig. 1(a). The 1D PC, comprised of a linear grating surface structure, was fabricated using a nanoreplica molding process approach that has been described in detail previously.²¹ Briefly, a silicon mold bearing a grating pattern was fabricated by electron-beam lithography and reactive ion etching, with surface area of 2 mm × 2 mm. Liquid ultra-violet curable epoxy (UVCP, NOA 85, Norland Product Inc.) was squeezed between the silicon mold and a transparent acrylic film and was solidified by exposing to UV light through the plastic substrate. Once separated from the silicon mold, the substrate film with the cured epoxy (refractive index, $n_{UVCP} = 1.46$) carried a grating pattern with a period of $\Lambda = 400$ nm, duty cycle of 60%, and a depth of $d = 60$ nm. The grating surface was coated with a 100 nm titanium dioxide (TiO₂) dielectric film using an electron beam evaporator. The TiO₂ thin film (refractive index, $n_{TiO_2} = 2.0$) provided light confinement for the GMRs. The design parameters were chosen to maximize the strength of optical resonance at the excitation wavelength and to provide strong local field intensity at the PC surface.

A schematic of the detection instrument is shown in Figure 1(b). The setup consists of a HeNe laser source with emission at $\lambda = 632.8$ nm, an optical chopper, a tunable mirror

^{a)}Electronic address: menglu@iastate.edu

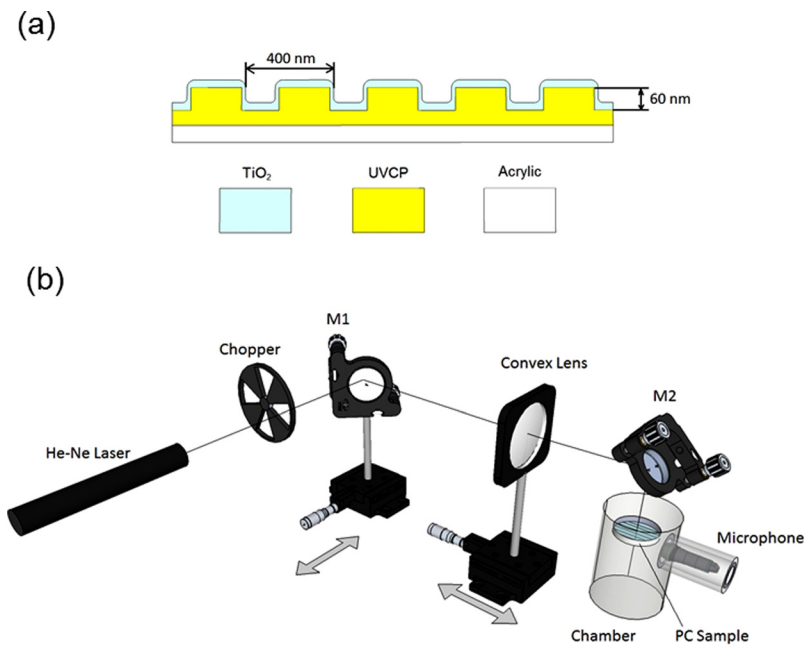


FIG. 1. (a) Schematic cross section of the PC structure (not to scale). The grating structure is fabricated using replica-molding process with period and duty cycle of 400 nm and 60%, respectively. (b) Complete optical layout of the experimental set-up. Linear polarized laser excitation at 632.8 nm was intensity modulated by a mechanical chopper wheel and reflected by a mirror (M1) that is translated horizontally to adjust the angle of incidence. A long-focus lens was used to focus the laser beam onto the PC sensor located on the topside of the PA chamber. The diameter of the focused laser spot was around 80 μm .

(M1) mounted on a translation stage, a convex lens, a second mirror (M2), and a PA analysis module (PAC 200 MTEC Photoacoustic Inc.) that incorporates the PC substrate. During the test, the output power of the HeNe laser was kept at 5 mW. The chopper modulated the laser emission with a square wave pattern at a frequency of 13 Hz. To excite a GMR at the desired wavelength (632.8 nm), the excitation light should illuminate the PC substrate at a specific angle of incidence. In the system, the mirror (M1) and the convex lens were utilized to tune the incident angle, defined in the direction perpendicular to the orientation of the grating. The convex lens with a focal length of 150 mm was fixed at a position so that its focal point was exactly on the sample. Translation of the M1 enabled adjustment of the incident angle from -7.2° to 7.2° . As the excitation light was efficiently coupled into the GMR, the intensified near field on the PC surface occurred and consequently generated a stronger photothermal effect.

The PA detection experiments require a sealed chamber to eliminate the ambient vibration noise. To combine the PC and the chamber, we attached the PC sensor onto an acrylic window that sealed the chamber with the PC facing the inside of the chamber. An acoustic transducer, a microphone (4176, Brüel & Kjær A/s), was connected to the chamber to measure photoacoustic pressure oscillations. During the experiments, light absorbing materials coated on the PCs absorbed light energy and generated pressure oscillations in the atmosphere of the chamber due to absorption induced heating. These pressure oscillations were converted to a voltage output by the microphone and were subsequently quantified using an oscilloscope (TDS2000, Tektronix). In the experiment, PA outputs were calculated by averaging voltage amplitudes in the waveforms obtained from the oscilloscope.

In order to characterize the enhancement performance of the fabricated PC, a PA detection experiment using a light absorbing dye was carried out on the PC substrate. The PC substrate was cleaned with isopropyl alcohol, de-ionized (DI) water, and dry N_2 , and the organic dye (Epolight 5262, Epolin Inc.) was dissolved in methanol and made up to

concentrations in the range from 50 $\mu\text{g}/\text{ml}$ down to 1 $\mu\text{g}/\text{ml}$. The dye solutions were drop-cast on the substrates and dried before use. To identify the resonant angle, we measured the laser transmission efficiency through the PC as a function of incident angle (θ_i) as shown in Figure 2, where the dip in the transmission curve corresponds to the resonant angle (θ_r), in this case $\theta_r = 3.5^\circ$. Plotted as the red curve in the same figure is the PA signal from 5 $\mu\text{g}/\text{ml}$ dye absorbed on the PC surface. Figure 2 clearly illustrates how the optical resonance (low transmission efficiency) results in a stronger PA output. After the subtraction of background signal, the PA signal at $\theta_r = 3.5^\circ$ is 5.8 V that is more than 10 \times higher than the PA signal measured away from this angle. Furthermore, Figure 3 shows the PA signals measured using a 2-fold dilution series of a total of six dye concentrations in the aforementioned range of concentration. In Figure 3, the red curve represents PA signals measured under resonance condition, when the GMR was excited at the angle of incidence of $\theta_r = 3.5^\circ$. As a reference, the black curve in Figure 3 shows the PA signal

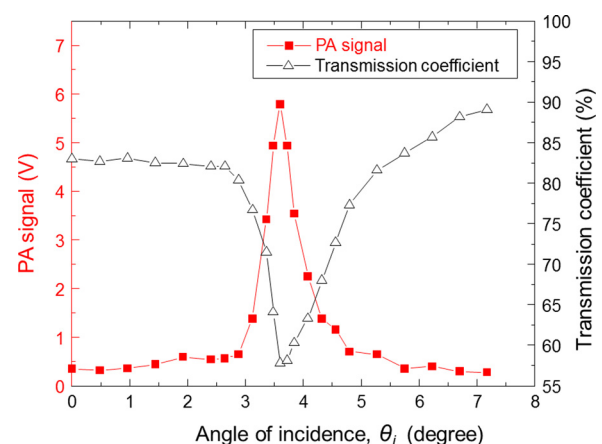


FIG. 2. A comparison of the PA signal (red square) to the normalized transmission coefficient (black triangle) measured as a function of incident angle tuned from 0° to 7.2° . The normalized transmission coefficient of PC substrate was measured using a TM-polarized HeNe laser source.

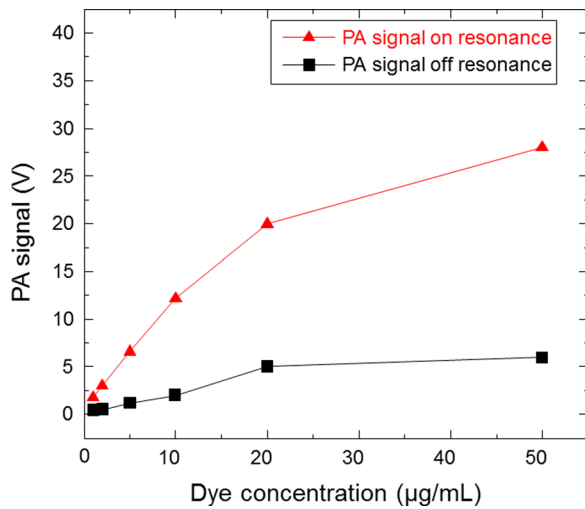


FIG. 3. PA signal intensity for a dilution series of absorbing dyes deposited on a PC substrate. The PC substrate was illuminated at 3.5° as the on resonance case (red triangle) and at 7° as the off resonance case (black square).

outputs of the dyes when the HeNe laser illuminated the PC under “off-resonance” condition ($\theta_i = 7^\circ$). At the dye concentrations below $20 \mu\text{g/ml}$, both curves vary linearly in terms of dye concentration. In this linear range, the sensitivity is $1.25 \text{ V}/(\mu\text{g/ml})$ when the PC is on resonance as compared to $0.18 \text{ V}/(\mu\text{g/ml})$, when it is off resonance, resulting in an averaged enhancement of 7-fold. Figure 3 clearly demonstrates that the PC enhancement provided easily distinguishable PA outputs and an extended range of quantification for the dyes at low concentrations. At higher concentrations, the PA signal started to saturate and the enhancement factor was reduced to

5.3 because the loss induced by the absorption of dye molecules quenched the PC resonance and reduced the PC enhancement factor.

Having demonstrated the PA signal enhancement of PC substrate to organic light absorbing molecules, we next exploited the PC resonance for the PA detection of metal NPs immobilized on the PC surface. Due to the localized surface plasmon resonance, the metal NPs exhibited tunable absorption in visible and near IR wavelength range.²² Finite difference time domain (FDTD) simulation was utilized to calculate the near field distributions upon the PC sensor, which was coated with metal nanoparticles. The cross-sectional views of electric field intensity for a gold nanoparticle (AuNP) on a flat acrylic substrate, a blank PC sensor, and an AuNP on PC sensor are shown in Figure 4(a). The dimensions of the simulated PC structure are specified in Figure 1(a) and the gold nanoparticle has an axial diameter of 25 nm and length of 60 nm. In the FDTD simulation, the incident field was set as a plane wave propagating towards the PC surface at the resonant wavelength of $\lambda_r = 632 \text{ nm}$ and the coupling angle of $\theta_r = 0^\circ$. The periodic boundary conditions were used in the grating plane to define the computational region. The scale bars on the right side represent resonant electric field intensity ($|\mathbf{E}|^2$) levels normalized with respect to the incident electric field intensity. As shown in Figure 4(a), the evanescent field within a hundred-nanometer range above the PC surface is significantly enhanced. The resonant field of the PC sensor is not significantly disturbed by the presence of the AuNP and the field intensity near the AuNP is further intensified due to the plasmonic resonance. Figure 4(b) compares the calculated absorption spectrum of AuNPs on PC and acrylic substrates. At the resonant wavelength, the

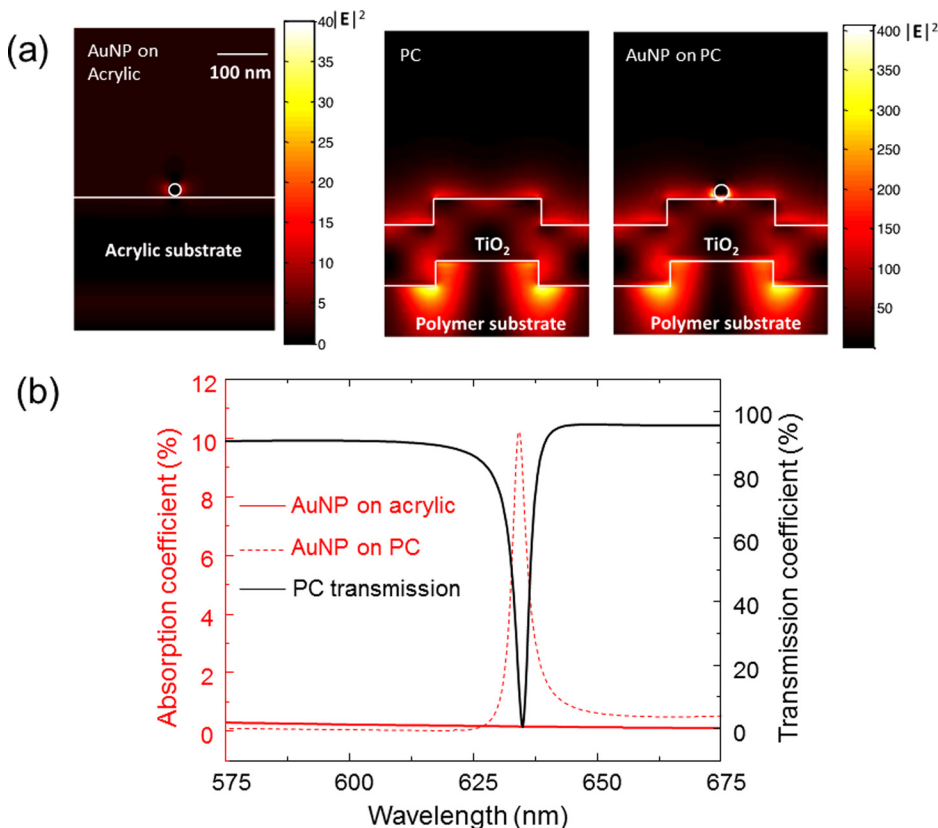


FIG. 4. (a) Spatial distribution of the simulated near-field intensity within a single period of the PC grating, for an AuNP on a flat acrylic substrate, a blank PC substrate, and an AuNP on a PC surface, respectively. The upper horizontal white lines indicate the substrate surfaces and the white circles represent the surface of the AuNP. (b) Calculated absorption spectra of AuNPs on acrylic and PC substrates. The modeled transmission spectrum shows the correlation between the GMR mode and the enhanced optical absorption of AuNPs on the PC sensor. The surface density of the AuNPs is $6.25 \text{ NPs}/\mu\text{m}^2$.

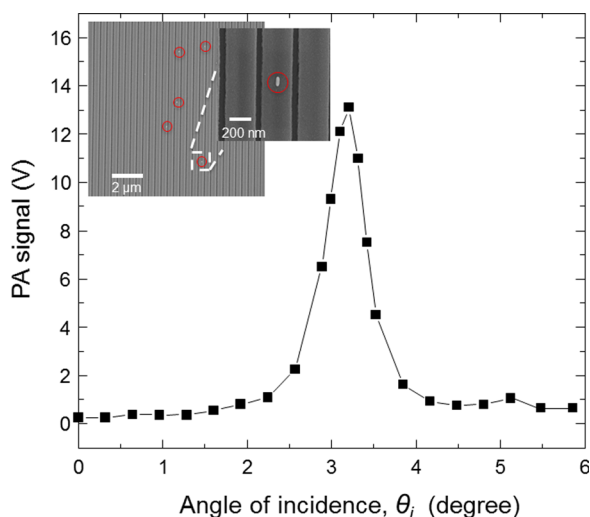


FIG. 5. Measured PA signal intensity of AuNPs on a PC surface as a function of incident angle between 0° and 6° . Inset: SEM image of the PC substrate with Au nanorods dispersed at 10^{10} NPs/ml.

absorption of AuNPs on the PC substrate becomes $60\times$ stronger than the same AuNPs on the planar acrylic substrate.

Detection of metal NPs was characterized by depositing gold nanorods onto the PC surface. Gold nanoparticle samples were prepared by suspending gold nanorods of approximately 25 nm axial diameter (A12-25-650, Nanopartz Inc.) in DI water. To deposit the AuNPs, $10\ \mu\text{l}$ spots of these samples were pipetted onto PC substrates and allowed to dry in air before measuring. A scanning electron microscopy image of PC coated with AuNPs at the concentration of 10^{10} NPs/ml is shown in the inset of Figure 5 where only a few nanorods are present within a $10\ \mu\text{m} \times 10\ \mu\text{m}$ area. Figure 5 illustrates the intensity of PA signal measured as a function of the incident angle of the excitation laser. The laser was scanned from $\theta_i=0^\circ$ to 7.2° and coupled into the GMR at $\theta_i=3.2^\circ$. Measured under resonant conditions, the intensity of PA signal is over 13 V that is $40\times$ stronger than the PA output (0.33 V) measured without utilizing the PC resonance.

The PC provides substantial increase in the PA output of AuNPs and also significant reduction in the PA detection limit. In order to demonstrate this, samples coated with AuNPs at a range of concentrations (10^{12} NPs/ml, 10^{11} NPs/ml, 10^{10} NPs/ml, and 10^9 NPs/ml) are measured for the PC illuminated on-resonance ($\theta_i=3.2^\circ$), off-resonance ($\theta_i=7^\circ$), and for the control acrylic slides. The measured PA signals with background subtracted are compared in Figure 6. The lowest detectable concentration on the acrylic substrate (10^{10} NPs/ml) is reduced by one order of magnitude to 10^9 NPs/ml on PC substrate. At higher concentrations, the amplification factor becomes weaker due to the quench of optical resonance caused by the absorption of AuNPs. The PC sensor offers the capability to detect less than 10 nanorods within a $100\ \mu\text{m}^2$ surface area.

In summary, a 1D PC substrate has been characterized for its capability to enhance the PA signal from light absorbers deposited onto the sensor surface. The PC sensor was incorporated into a PA measurement chamber and illuminated by a HeNe laser with the angle of incidence tuned to excite the GMR. The strengthened local field associated with

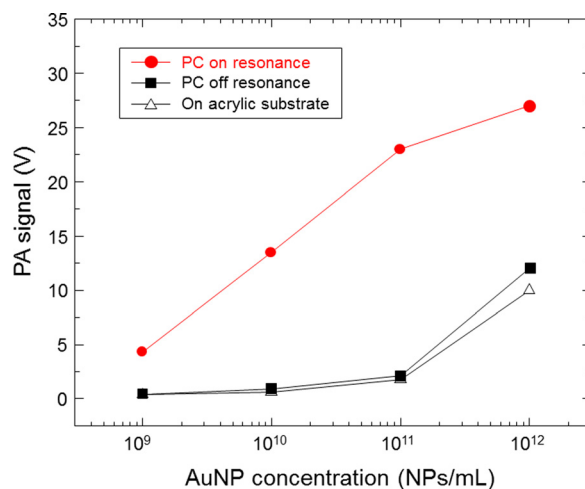


FIG. 6. PA signal intensity for a dilution series of gold nanoparticles deposited on a PC substrate and an acrylic substrate, respectively. The PC substrate was illuminated at 3.2° for on-resonance (red circle) and at 7° for off-resonance (black square).

the resonant mode increased the optical absorption of analytes deposited on the PC and resulted in an enhanced PA signal by factors of $10\times$ and $40\times$ for the organic light absorber and the gold nanorods, respectively. The enhanced PA signal consequently reduced the detection limit of metal nanoparticles by one order of magnitude. The PC substrate demonstrated here represents a powerful and practical approach for highly sensitive PA detection and would be improved further for sensors produced over substantially large surface area with higher quality factors. In the future work, this technique will be exploited to facilitate the quantification of metal nanoparticles functionalized with recognition molecules, enabling a promising approach for diagnostic test and environmental monitoring.²³

This research was supported by the start-up funding from the Iowa State University. The authors would like to acknowledge Dr. Wai Y. Leung of Microelectronics Research Center at Iowa State University for the technical supports.

¹A. Rosencwaig, *Photoacoustics and Photoacoustic Spectroscopy* (Wiley, New York, 1980).

²J. F. McClelland, *Anal. Chem.* **55**(1), 89A–105A (1983).

³A. C. Tam, *Rev. Mod. Phys.* **58**(2), 381–431 (1986).

⁴H. Zhang, K. Maslov, G. Stoica, and L. Wang, *Nat. Biotechnol.* **24**(7), 848–851 (2006).

⁵A. Miklos, P. Hess, and Z. Bozoki, *Rev. Sci. Instrum.* **72**, 1937–1955 (2001).

⁶V. Koskinen, J. Fonsen, K. Roth, and J. Kauppinen, *Vib. Spectrosc.* **48**(1), 16–21 (2008).

⁷M. Hippler, C. Mohr, K. A. Keen, and E. D. McNaghten, *J. Chem. Phys.* **133**(4), 044308 (2010).

⁸A. Kachanov, S. Koulikov, and F. K. Tittel, *Appl. Phys. B* **110**, 47–56 (2013).

⁹A. A. Kosterev, Yu. A. Bakhrkin, R. F. Curl, and F. K. Tittel, *Opt. Lett.* **27**(21), 1902–1904 (2002).

¹⁰H. Lin, Y. Zou, and J. Hu, *Opt. Lett.* **37**(8), 1304–1306 (2012).

¹¹S. S. Wang and R. Magnusson, *Appl. Opt.* **32**(14), 2606–2613 (1993).

¹²S. Fan and J. D. Joannopoulos, *Phys. Rev. B* **65**(23), 235112 (2002).

¹³Y. Ding and R. Magnusson, *Opt. Express* **12**(23), 5661–5671 (2004).

¹⁴D. Neuschaefer, W. Budach, C. Wanke, and S. D. Chibout, *Biosens. Bioelectron.* **18**, 489–497 (2003).

¹⁵V. Chaudhery, S. George, M. Lu, A. Pokhriyal, and B. T. Cunningham, *Sensors Journal* **13**, 5561–5584 (2013).

- ¹⁶C.-S. Huang, S. George, M. Lu, V. Chaudhery, R. Tan, R. C. Zangar, and B. T. Cunningham, *Anal. Chem.* **83**(4), 1425–1430 (2011).
- ¹⁷J. H. Lin, C. Y. Tseng, H. C. Kan, and C. C. Hsu, *Opt. Express* **21**(20), 24318–24325 (2013).
- ¹⁸A. Pokhriyal, M. Lu, C.-S. Huang, S. C. Schulz, and B. T. Cunningham, *Appl. Lett.* **92**(12), 121108 (2010).
- ¹⁹A. Pokhriyal, M. Lu, V. Chaudhery, C.-S. Huang, S. Schulz, and B. T. Cunningham, *Opt. Express* **18**(24), 24793–24808 (2010).
- ²⁰J.-N. Liu, M. V. Schulmerich, R. Bhargava, and B. T. Cunningham, *Opt. Express* **19**(24), 24182–24197 (2011).
- ²¹M. Lu, S. S. Choi, U. Irfan, and B. T. Cunningham, *Appl. Lett.* **93**(11), 111113 (2008).
- ²²J. N. Anker, W. P. Hall, O. Lyandres, N. C. Shah, J. Zhang, and R. P. Van Duyne, *Nature Mater.* **7**, 442–453 (2008).
- ²³K. A. Willets and R. P. Van Duyne, *Annu. Rev. Phys. Chem.* **58**, 267–297 (2007).